



HAL
open science

Direct physical modelling and scene reconstruction in order to assess the performance from a new concept of active imaging: Mosaic active imaging system

Emmanuelle Thouin, Marie-Thérèse Velluet, Dominique Hamoir, Laurent Hespel, François Malgouyres, Xavier Briottet

► To cite this version:

Emmanuelle Thouin, Marie-Thérèse Velluet, Dominique Hamoir, Laurent Hespel, François Malgouyres, et al.. Direct physical modelling and scene reconstruction in order to assess the performance from a new concept of active imaging: Mosaic active imaging system. 10th International IR Target and background modeling & simulation workshop, 2014, Ettlingen, Germany. hal-01486854

HAL Id: hal-01486854

<https://hal.science/hal-01486854>

Submitted on 10 Mar 2017

HAL is a multi-disciplinary open access archive for the deposit and dissemination of scientific research documents, whether they are published or not. The documents may come from teaching and research institutions in France or abroad, or from public or private research centers.

L'archive ouverte pluridisciplinaire **HAL**, est destinée au dépôt et à la diffusion de documents scientifiques de niveau recherche, publiés ou non, émanant des établissements d'enseignement et de recherche français ou étrangers, des laboratoires publics ou privés.

Direct physical modelling and scene reconstruction in order to assess the performance from a new concept of active imaging: Mosaic active imaging system.

Emmanuelle Thouin^{a,b}, Marie -Thérèse Velluet^c, Dominique Hamoir^a, Laurent Hespel^a, Francois Malgouyres^d and Xavier Briottet^a

^aONERA - The French Aerospace Lab, 2 av Edouard Belin, F-31055 Toulouse, France;

^bUniversity of Toulouse, ISAE - Institut "Supérieur de l'Aéronautique et de l'Espace", F-31055 Toulouse, France;

^cONERA - The French Aerospace Lab, 29 Avenue de la Division Leclerc, F-92320 Châtillon, France;

^dIMT CNRS UMR5219, University of Toulouse, Toulouse, France

ABSTRACT

Active imaging can be used for surveillance or target identification at long range and low visibility conditions. Its principle is based on the illumination of a scene with a pulsed laser which is then backscattered to the sensor. The signal to noise ratio and contrast of the object over the background are increased in comparison with passive imaging. Even though, range and field of view (FOV) are limited for a given laser power. A new active imaging system presented here aims at overcoming this limitation. It acquires the entire scene with a high-speed scanning laser illumination focused on a limited region, whereas at each scan the full frame active image is acquired. The whole image is then reconstructed by mosaicking all these successive images. A first evaluation of the performance of this system is conducted by using a direct physical model. This end-to-end model, realistic in terms of turbulence effects (scintillation, beam wandering ...), gives us a sequence of images a synthetic scenes. After presenting this model, a reconstruction method of the total scene is described. And the performances of this new concept are compared to those of a conventional flash active camera by using usual metrics (SNR, MTF ...). For various mean laser powers, we quantify the gains expected in terms of range and field of view of this new concept.

Keywords: Active Imaging, laser imaging, image reconstruction, physical modelling, optimization problem

1. INTRODUCTION

Flash active imaging can be used for surveillance or target identification at long range and low visibility conditions. Its principle is based on the illumination of a scene with a pulsed laser which is then back-scattered to the sensor. When compared to passive imaging, the signal to noise ratio and contrast of the object over the background are increased. Even though, range and Field of View (FOV) are limited for a given peak laser power. In order to overcome these limitations, a new concept of active imaging system has been developed at Onera. It is based on the acquisition of the entire scene with a high-speed scanning laser illumination on a limited region to increase the irradiance, whereas at each scan the full frame active image is acquired. The whole image is then reconstructed by mosaicking from composite image of all these successive images (Fig. 1). In order to assess the performance of this new active imaging method and compare with the conventional one's, a better knowledge of the propagation through the atmosphere of low divergence laser beam and a prior work to restore the whole image from such a mosaic are required.

This paper gives an overview on the status of this work. A first evaluation of the performance of this new system is conducted by using an end-to-end modeling. A direct model including propagation of the illumination



Figure 1. Left to right: the mosaic laser imaging process, the ideal image we want to estimate, a reduced part of the field of view with a single laser flash, the image composed from all laser shots where each pixel is assigned with its maximum intensity over all of them.

beam, backscattering on the object and forward propagation to the instrument is performed to create the image recorded by the detector. The inverse chain is then described to retrieve the total scene. The MAP is used to restore the image, it corrects the artefacts introduced by the mosaic active imaging concept. Modeling and restoration processing are described in Section 2. Finally in Section 3, the results are then compared to the performance of a full scene active imaging system. For each scene, we measure the Signal to Noise Ratio (SNR), the profile image and the contrast. The influence of the different physical parameters on the quality of the image is also considered.

2. MOSAIC ACTIVE IMAGING

2.1 Forward Physical Modelling

The end-to-end model presented here is based on an initial work on the flash laser imaging system published in [1]. It includes all the physical components: the laser, the target, the outbound and inbound atmospheric paths and the camera. The model takes into account the principal phenomena: the scintillation, the beam spreading, the beam wander, the beam jitter, the speckle, the interaction with the target, the filtering by the receiver (optical and detector) and the camera noises. It is based on an approach for laser beam propagation simulation through turbulence that is simpler and faster than the commonly used numerical end-to-end model.

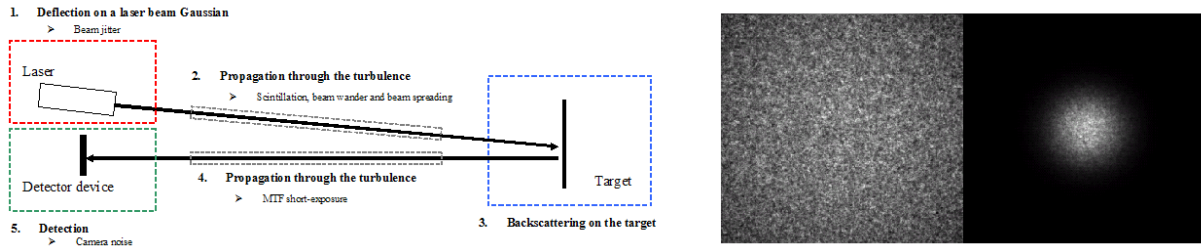


Figure 2. On left : Approach adopted to study a mosaic active imaging system. On right: Results illumination patterns generated by simulation: beam divergent (left), beam less divergent (right). The images were taken at measured C_n^2 value of $1.10^{-14} m^{-2/3}$. $L = 1 km$, $\lambda = 1,57 \mu m$ and an $8,5 mrad$ FOV camera.

The approach adopted to simulate images from a mosaic active imaging system is shown in figure 2: 1- The source is assumed to be a gaussian laser beam. 2- Due to its propagation through the atmosphere. The laser beam intensity distribution is non uniform. To simulate this instantaneous turbulence effects on the propagated laser beam, we have developed a method based on the dissociation of scintillation from beam spreading and beam wander which appears to be justified in weak perturbation regime [2]. Examples of the instantaneous beam profiles generated by our simplified model are shown in Figure 2. 3- The reflected intensity is obtained by multiplying the laser map with the target image appropriately selected and scaled. 4- The reflected laser

beam propagation is retrieved by applying the short-exposure Modulation Transfer Function (MTF). 5- Then, we apply the detector MTF and we add different camera noises. The output image is re-sampled in order to have the same dimensions as the camera array.

The validity of this model was checked by comparing the results to those obtained with a numerical end-to-end propagation model called Pilot (Propagation and Imaging, Laser and Optical through Turbulence) based on a split step algorithm and developed at Onera [3]. A first validation by comparison of the mean amplitude, the Power Spectral Density (PSD) and the probability distribution with Pilot has been presented in [2]. In the case of spherical wave in the weak perturbation regime, a good accordance between both methods is presented. A second validation by comparison of the beam radii and the scintillation index with Pilot is being published.

The work allowed us to estimate the difficulties of total scene restoration and qualitatively pre-evaluate the influence of physical parameters on the final results.

2.2 Images reconstruction

The restoration of the whole scene from k acquired images with this new active imaging system is an inverse problem. The observed image v_k of the ideal scene u (i.e. the one that would have been obtained with a non gaussian illumination) at the focal plane of the detector is given by:

$$v_k = M_k u + n \quad (1)$$

where n is a corruptive noise process and M_k an operator. Note that the operator M_k needs to be estimated, $\forall k \in \{1, \dots, K\}$, because all the acquisition parameters are not essentially the same as soon as they include atmospheric perturbations. The restoration algorithm consists in alternatively estimate these acquisition parameters and the image. The estimation of the whole image relies on the minimization (or maximization) of a criterion.

To solve this problem, we first have considered a fine noise model that accounts for both photonic and detector noises. The photon noise follows Poisson statistics and the detector noise follows Gaussian, and approximately stationary, statistics. We assume a Gaussian prior on the acquisition parameters and a quadratic-linear prior on the distribution of images, recently applied to imaging through turbulence [5]. Based on these assumptions and for a given number k of acquired images v_k , the MAP estimation is calculated by minimizing the criterion $J_1(u)$ defined as follows:

$$J_1(u) = \sum_k \frac{|v_k - M_k u|^2}{2\sigma^2(k)} + \mu\delta^2 \sum_{l,m} \phi(\nabla u(l, m)/\delta) \quad (2)$$

where $\phi(x) = |x| - \ln(1 + |x|)$ and $\sigma^2(k)$ is the sum of the photon noise and the detector noise variances. The global factor μ and the threshold δ are adjusted according to the noise level and the structure of the object. The criterion of Eq.(2) is minimized numerically to obtain the joint MAP estimate for the ideal image u . The minimization is performed by a conjugate-gradient method. This work allowed us to give a first solution to this problem. We observe that the reconstruction method behaves globally well. The structures are well preserved, even between domes where the SNR is cover about data is less precise.

3. SIMULATION RESULTS

The simulations detailed in this section have the following system parameters: an laser energy at $\lambda = 1, 57\mu m$ of $14mJ$, an $2, 3 \times 2, 3m$ object size, and an $8, 5mrad$ FOV camera. The object of interest typically lies between $1km$ and $4km$ from the imaging system. The divergence of laser beam for the conventional flash system is $5mrad$. To compare the performance of this new concept to those of a conventional flash active imaging camera we choose to have the same mean laser power. Also, for the new concept the divergence of laser beam changes of $1, 2mrad$, $800\mu rad$ and $300\mu rad$ at a propagation distance of $1, 1, 5$ and $4km$, respectively. To cover the totality of the surface of the target, we generate $k = 41$ scans. The comparison of those concepts is done by using usual metrics. We study the influence of the different physical parameters on the quality of the image. For each sequence, we

measure the Signal to Noise Ratio (SNR), the image profile and the contrast. The evaluation is conducted on the images patterns and using the method provided in Section 2.2.

In figure 3, the distance between the imaging system and the object of interest is $1,5km$, the beam laser divergence of the mosaic active imaging system is $div. = 800\mu rad$ and we considered several values of C_n^2 , $C_n^2 = 1.10^{-15}$, 5.10^{-14} and $1.10^{-13}m^{-2/3}$. From left to right: we provide for each image, the ideal one (image without turbulence which is sum of 40 images to reduce speckle effects, with a uniform intensity distribution), the image with conventional flash system, the resulting image of scan system (where each pixel assigned with its maximum intensity of scanned images), and reconstruction image from the second method described in Section 2.2. We observe that the images change with increasing values of C_n^2 . The signal is limited by the detector noise. In figure 4, the object of interest is placed at $1,5km$ and $4km$ from the imaging system and $C_n^2 = 1.10^{-15}m^{-2/3}$.

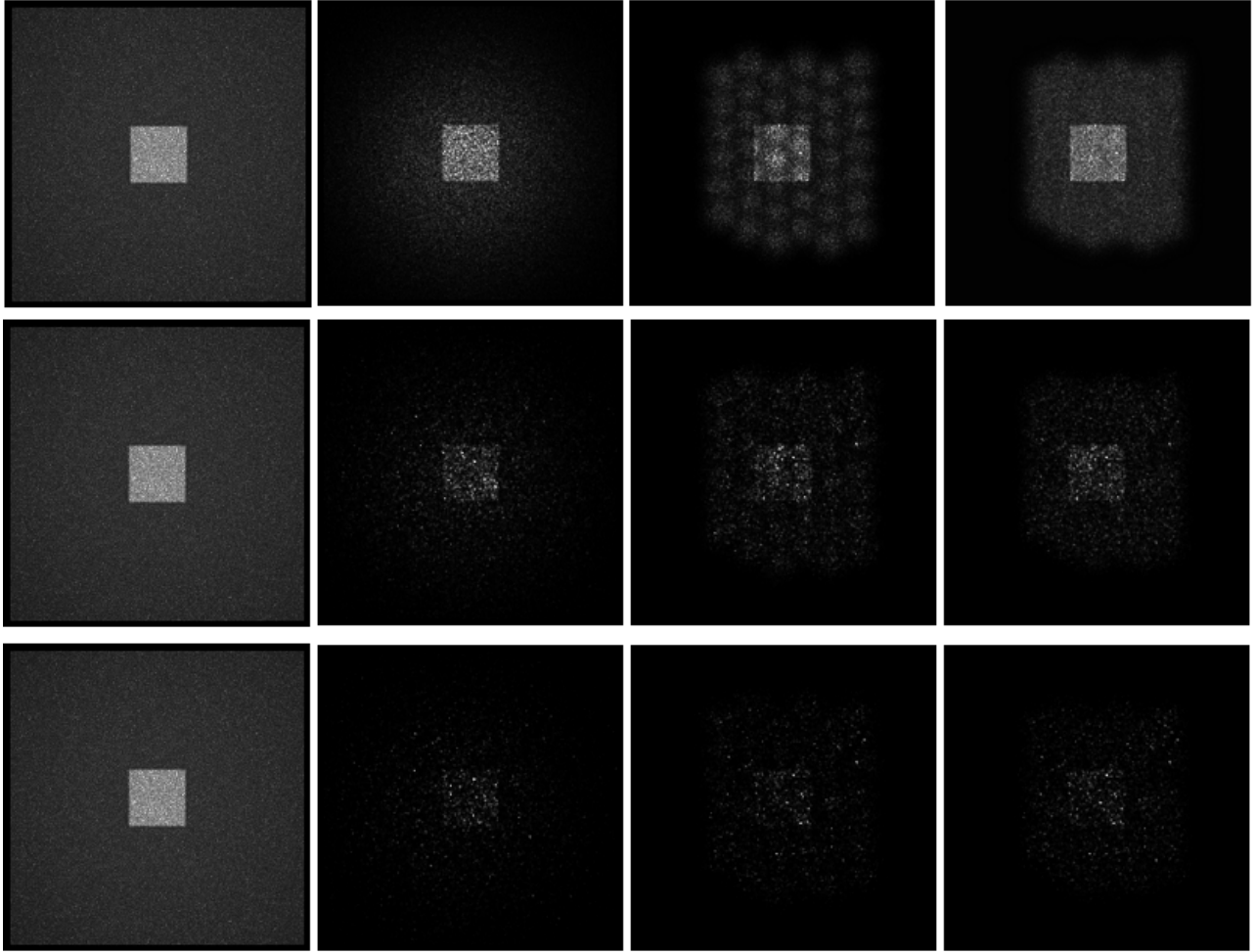


Figure 3. Left to right: The ideal image; Image with conventional flash system; Resulting image of scan system, where each pixel assigned with its maximum intensity of scanned images; Reconstruction with the algorithm using conjugate-gradient. Top to bottom: The images were taken at measured C_n^2 value of 1.10^{-15} , 5.10^{-14} and $1.10^{-13}m^{-2/3}$. $L = 1,5km$, $\lambda = 1,57\mu m$ and $div. = 800\mu rad$.

The metrics cited below are determined on the object of interest, that means on an uniform white board or on a bar target. The albedo of the board equals 0.5, and those white bar is 0.5 and the those of black bar is 0.3. We define the SNR as the ratio of the mean intensity of the white board and its standard deviation: $SNR = \frac{\langle I \rangle}{\sigma_I}$.

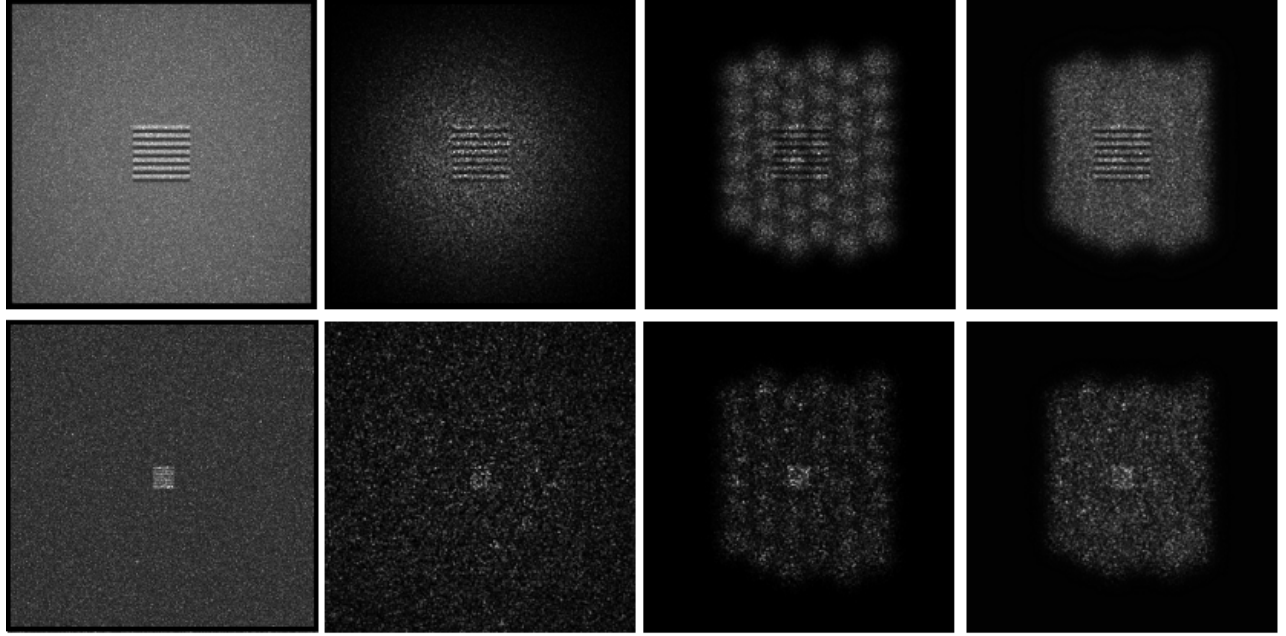


Figure 4. Left to right: The ideal image; Image with conventional flash system; Resulting image of scan system, where each pixel assigned with its maximum intensity of scanned images; Reconstruction with the second algorithm using conjugate-gradient. The images were taken at measured C_n^2 value of $1.10^{-15}m^{-2/3}$. Top to bottom: $L = 1, 5$ and $4km, \lambda = 1, 57\mu m$

The SNR were calculated for classical system, scan system and system after image processing image processing. Results are summarized in Table 1. We observe a decrease of SNR with the propagation distance and the C_n^2 . For each scene, an SNR is higher for the reconstruction. When C_n^2 is higher than 5.10^{-14} the improvement is quite low.

$L (km)$	1				1,5				4			
$C_n^2 (m^{-2/3})$	1.10^{-15}	1.10^{-14}	5.10^{-14}	1.10^{-13}	1.10^{-15}	1.10^{-14}	5.10^{-14}	1.10^{-13}	1.10^{-15}	1.10^{-14}	5.10^{-14}	1.10^{-13}
SNR conform classical system	11,41	8,24	7,83	5,96	9,29	7,78	2,73	1,78	3,37	2,27	1,11	1,07
SNR conform scan system	10,35	7,64	7,47	5,86	6,54	5,02	2,37	1,66	4,23	4,10	1,50	1,15
SNR conform reconstruction	16,60	10,92	9,51	6,97	16,39	10,18	2,85	1,80	6,29	6,09	1,50	1,16

Table 1. Comparison of the mosaic active system with the conventional active system. Signal-to-noise ratio is defined as the power ratio between the mean of signal and the variance of the signal . The measures were made only on the target.

Concerning the bar chart, we have studied the evolution of the contrast with distance and C_n^2 . For each bar chart, we plot the average profile of object along the horizontal axis. One result is presented figure 5 and Table 2. We define contrast as the ratio of intensity difference and intensity sum: $Contrast = \frac{(\langle I_{max} \rangle - \langle I_{min} \rangle)}{(\langle I_{max} \rangle + \langle I_{min} \rangle)}$ with $\langle I_{max} \rangle$ and $\langle I_{min} \rangle$ representing the mean highest and lowest intensity. The contrasts were calculated for classical system, scan system and system after image processing (reconstruction). At $1km$, the contrast is similar for those methods. When the propagation distance is $1, 5km$, the contrast is slightly better for reconstruction. We have to continue the study on full validation of the gains of the new system by increasing the C_n^2 , propagation distances and by a optimization scans.

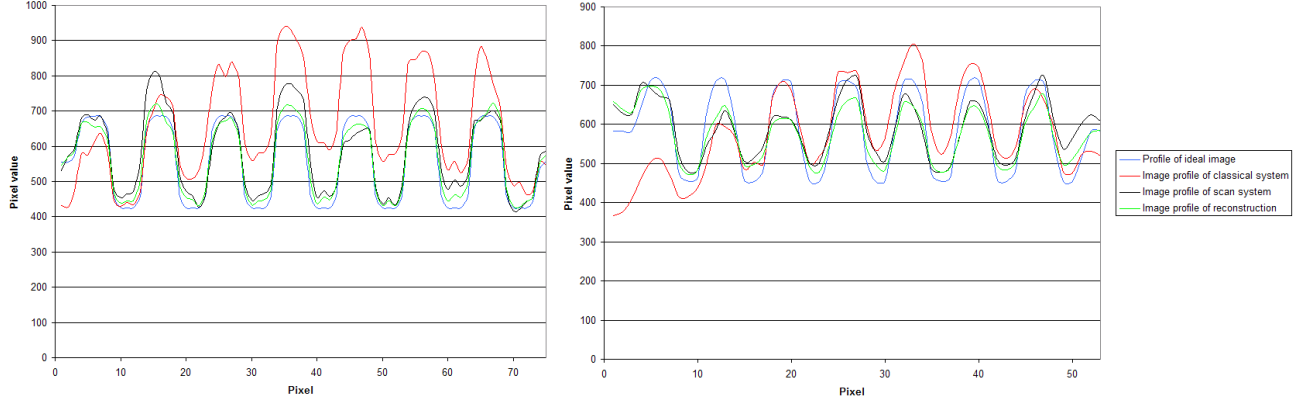


Figure 5. Comparison of image profiles of the scene from the mosaic active system with those of the conventional system. The image profiles of the scene taken at measured C_n^2 value of $1.10^{-15} m^{-2/3}$. Left to right: $L = 1 km$; $L = 1.5 km$

	Contrast 1km	Contrast 1,5km
Ideal profile	0,233	0,222
Classical system	0,231	0,160
Scan system	0,226	0,148
Reconstruction	0,228	0,192

Table 2. Comparison of the mosaic active system with the conventional active system. Evolution of the contrast with distance with the propagation distance. The measures were made only on the target

4. CONCLUSION

To assess the capacity of a new concept of active imaging to improve range in comparison with usual concept, we have developed an end-to-end model including a post processing. Then, a method to restore the observed scene are proposed and compared. It allows reconstruction globally well the total scene of a mosaic active imaging system. Finally, the performances of this new concept are confronted to those of a conventional flash active camera. We quantified gains in terms of SNR and contrast of this new concept for various mean laser powers, propagation distances and C_n^2 . The new concept allows the use of less powerful laser but faster repetition rate. For example, at 1,5km the classical system requires 14mJ at 10Hz, and the new concept only 800μJ at 400Hz. However, the image processing is necessary for this new concept.

Future work, we plan to continue this sensibility study by increasing the C_n^2 , propagation distances and by an optimization of scans process. Also, we plan to validate the model results with experiments results from an active imaging system.

ACKNOWLEDGMENTS

We would like to thank Dr. Laurent Mugnier for his extraordinary support in this images reconstruction work. We thank him for valuable discussion.

REFERENCES

1. O. Steinvall, I. Renhorn, J. Ahlberg, H. Larsson, D. Letalick, E. Repasi, P. Lutzmann, G. Anstett, D. Hamoir, L. Hespel, Y. Boucher, "ACTIM: An EDA initiated study on active spectral imaging," SPIE Defence+Security Europe, Proc. SPIE 7835A, (2010).
2. L. Hespel, M.T. Velluet, A. Bonnefois, N. Rivière, M. Fraces, D. Hamoir, B. Tanguy, B. Duchenne, J. Isbert, "Comparison of a physics-based BIL simulator with experiments ISPDI," Proc. SPIE 7382, (2009)

3. M.-T. Velluet, V. Michau, T. Fusco, J.M. Conan., J.M. Conan., "Coherent illumination for wavefront sensing and imaging through turbulence," Proc. Of SPIE Vol. 6708 670808-1, (2007).
4. J.M. Martin, S.M. Flatté., "Intensity images and statistics from numerical simulation of wave propagation in 3-d random media," Appl.Opt. 27(11), pp. 2111-2126, (1988).
5. R. L. Fante, "Electromagnetic beam propagation in turbulent media," Proc. IEEE 63, 1669-1692, (1975).
6. L. I. Rudin and al., "Nonlinear total variation based noise removal algorithms," Physica D Vol. 60 259-268, (1992).
7. L. M. Mugnier, T. Fusco, J-M. Conan, "MISTRAL: a myopic edge-preserving image restoration method, with application to astronomical adaptive-optics-corrected long-exposure images," J. Opt. Soc. Am. A Vol. 21, No. 10, (2004).